Journal of Biomechanics 141 (2022) 111200

Contents lists available at ScienceDirect

Journal of Biomechanics

journal homepage: www.elsevier.com/locate/jbiomech

Sensitivity analysis guided improvement of an electromyogram-driven lumped parameter musculoskeletal hand model

Robert Hinson Jr. [a,b], Katherine Saul [c], Derek Kamper [a,b], He Huang [a,b,*]

[a] UNC-NC State Joint Department of Biomedical Engineering, North Carolina State University, Raleigh, NC 27695, United States
[b] UNC-NC State Joint Department of Biomedical Engineering, University of North Carolina at Chapel Hill, Chapel Hill, NC 27599, United States
[c] Department of Mechanical and Aerospace Engineering, North Carolina State University, Raleigh, NC 27695, United States

ARTICLE INFO

Keywords:
Musculoskeletal modeling
Optimization
Upper limb
Rehabilitation

ABSTRACT

EMG-driven neuromusculoskeletal models have been used to study many impairments and hold great potential to facilitate human–machine interactions for rehabilitation. A challenge to successful clinical application is the need to optimize the model parameters to produce accurate kinematic predictions. In order to identify the key parameters, we used Monte-Carlo simulations to evaluate the sensitivities of wrist and metacarpophalangeal (MCP) flexion/extension prediction accuracies for an EMG-driven, lumped-parameter musculoskeletal model. Four muscles were modeled with 22 total optimizable parameters. Model predictions from EMG were compared with measured joint angles from 11 able-bodied subjects. While sensitivities varied by muscle, we determined muscle moment arms, maximum isometric force, and tendon slack length were highly influential, while passive stiffness and optimal fiber length were less influential. Removing the two least influential parameters from each muscle reduced the optimization search space from 22 to 14 parameters without significantly impacting prediction correlation (wrist: 0.90 ± 0.05 vs 0.90 ± 0.05, p = 0.96; MCP: 0.74 ± 0.20 vs 0.70 ± 0.23, p = 0.51) and normalized root mean square error (wrist: 0.18 ± 0.03 vs 0.19 ± 0.03, p = 0.16; MCP: 0.18 ± 0.06 vs 0.19 ± 0.06, p = 0.60). Additionally, we showed that wrist kinematic predictions were insensitive to parameters of the modeled MCP muscles. This allowed us to develop a novel optimization strategy that more reliably identified the optimal set of parameters for each subject (27.3 ± 19.5%) compared to the baseline optimization strategy (6.4 ± 8.1%; $p = 0.004$). This study demonstrated how sensitivity analyses can be used to guide model refinement and inform novel and improved optimization strategies, facilitating implementation of musculoskeletal models for clinical applications.

1. Introduction

Computational neuromusculoskeletal models have been developed to investigate various aspects of the human neuromusculoskeletal system in healthy and impaired populations. Recently, researchers have attempted to extend the application of musculoskeletal models beyond the study and explanation of impairments to include treatment as well. For example, musculoskeletal models have been successfully implemented as human–machine interfaces (HMIs) for control of both upper (Blana et al., 2020; Crouch and Huang, 2016; Pan et al., 2018; Sartori et al., 2018) and lower (Eilenberg et al., 2010) extremity prostheses, HMIs for control of exoskeletons (Durandau et al., 2019), test platforms for surgical planning (Delp et al., 1990; Rajagopal et al., 2020), guides for therapy to relieve medial knee pain during gait due to the osteoarthritis (Fregly et al., 2007), and provide insights into ankle sprains (Boey et al., 2022), ACL reconstruction results (Kotsifaki et al., 2022), and gait (Valente et al., 2013) for clinical application.

While these applications are encouraging, direct clinical employment of musculoskeletal modeling remains rare. One reason for this paucity of clinical translation is the challenge presented by model personalization. While generic musculoskeletal models help elucidate mechanisms of disorders and impairments, the anatomy, physiology, and neural control are unique for each individual and generic models may lack the predictive accuracy needed for clinical application (Zuk et al., 2018). Unfortunately, customization of parameters describing excitation-activation dynamics, muscle properties, and musculoskeletal geometry is incredibly challenging (Bueno and Montano, 2017; Davico et al., 2020; de Groote et al., 2010; Hoang et al., 2019; Manal et al.,

* Corresponding author at: North Carolina State University, Campus Box 7115, Raleigh, NC 27695-7115.
E-mail address: hhuang11@ncsu.edu (H. Huang).

https://doi.org/10.1016/j.jbiomech.2022.111200
Accepted 11 June 2022
Available online 16 June 2022

2002; Modenese et al., 2016; Pizzolato et al., 2015; Saxby et al., 2020). Many model parameters are not measurable, either directly or indirectly, thus leading researchers to utilize numerical optimization strategies to approximate parameter values for individuals (Fregly, 2021). As more parameters are included in the model, however, identification of an optimal set of values becomes increasingly challenging due to increased computational complexity and potential for finding local rather than global minima.

In order to overcome the challenges presented by model optimization, researchers have performed sensitivity analyses on musculoskeletal models (Redl et al., 2007; Scovil and Ronsky, 2006). Such analyses aim to determine the relative contributions of different parameters to model performance to determine appropriate model complexity. In the existing literature, many of these studies have focused on lower extremity and gait models. They have tended to evaluate sensitivity based on the impact of a parameter on model force generation (Ackland et al., 2012; Bujalski et al., 2018). As models are more frequently used in clinical and HMI applications to predict kinematics, it is important to perform sensitivity analyses directly on kinematics instead of an intermediate quantity like muscle force due to the nonlinearity of musculoskeletal models (Fregly, 2021).

In this study we sought to perform a sensitivity analysis of a Hill-type (Zajac, 1989) lumped-parameter upper extremity musculoskeletal model previously developed to use surface electromyograms (EMG) to predict wrist flexion/extension and metacarpophalangeal (MCP) flexion/extension (Crouch and Huang, 2016). While the feasibility of real-time control using this model has been demonstrated (Crouch et al., 2018; Crouch and Huang, 2017), showing its potential for control of upper extremity rehabilitation devices with a limited number of degrees of freedom (e.g., prosthesis control), efficient optimization for individuals remains a significant barrier to implementation outside of a research setting. We sought to determine model sensitivity to changes in Hill-type and musculoskeletal geometry parameter values. Based on existing literature, we hypothesized that while model prediction accuracy sensitivity would be muscle-dependent, it would be most influenced by maximum isometric force, tendon slack length, and optimal fiber length (Ackland et al., 2012; Bujalski et al., 2018; Redl et al., 2007). Furthermore, we explored how such an analysis can be applied to guide model designs and develop novel optimization strategies via elimination of parameters that displayed limited influence without sacrificing accuracy to make implementation outside of research settings more feasible.

2. Methods

2.1. Subjects

The experimental protocol was approved by the University of North Carolina at Chapel Hill Institutional Review Board. Eleven able-bodied subjects (6 male, 5 female, ages 18–31 years, right hand dominant) were recruited in the study. Subjects provided informed consent before participating.

2.2. Experimental design and data collection

Subjects performed 5 different motions while holding their dominant upper extremity with the elbow flexed to 90° and the forearm in a neutral posture: isolated MCP flexion/extension, with fixed and variable speed; isolated wrist flexion/extension, with fixed and variable speed; and simultaneous wrist and MCP flexion/extension at a variable speed. During fixed-speed movements subjects alternated between maximum flexion, relaxation, and maximum extension at a fixed tempo (0.25 Hz). A metronome set to 1 beat per second was used to provide subjects feedback when to switch to the next sequence in the cycle. Subjects moved at self-selected speeds and directions during variable-speed trials. Each motion was performed twice for a minimum of 30 s, resulting in 10 trials per subject (5 movement types × 2 repetitions).

Kinematic and EMG data were recorded synchronously during each trial. Four bipolar surface EMG electrodes (Biometrics, Newport, UK) were placed over the *extensor carpi radialis longus* (ECRL), *extensor digitorum communis* (EDC), *flexor carpi radialis* (FCR), and *flexor digitorum superficialis* (FDS). Each muscle was identified via palpation and anatomical reference. The EMG data were sampled at 960 Hz, high-pass filtered at 40 Hz, rectified, enveloped, and then low-pass filtered at 6 Hz (Crouch and Huang, 2016). Both filters were 4th-order digital Butterworth filters with zero phase shift. Processed EMG data were normalized using subjects' peak values from maximum voluntary contraction data for each muscle. Normalized EMG data were down-sampled to 120 Hz and converted to muscle activations (Lloyd and Besier, 2003).

Fourteen reflective markers were placed on anatomical landmarks of the hand and forearm to track wrist and MCP flexion/extension motion (Fig. 1). Three-dimensional marker position data were obtained at 120 Hz with a motion capture system (Vicon Motion Systems Ltd., UK). Marker data were low-pass filtered at 6 Hz (4th-order Butterworth, zero-phase). Joint angles were calculated from the filtered marker data in OpenSim (Delp et al., 2007) via inverse kinematics using a musculoskeletal model modified to include the 2nd through 5th MCP joints (Crouch and Huang, 2016; Holzbaur et al., 2005).

2.3. Subject-specific model generation

A previously described lumped-parameter, Hill-type musculoskeletal model (Crouch and Huang, 2016) was optimized to predict wrist and MCP flexion/extension angles from EMG inputs for each subject. The model includes 6 parameters per muscle: optimal fiber length (l_{opt}), maximum isometric force (F_{max}), moment arm at the wrist joint (ma_{wrist}), moment arm at the MCP joint (ma_{mcp}), fiber length at 0° ($l_{\theta=0}$), and passive stiffness (K). For the wrist flexor and extensor muscles, which do not cross the MCP joint, the MCP moment arm was set to zero, resulting in 22 optimizable parameters. Fig. 2 shows a representation of the model.

Parameters were optimized via minimization of the sum of squared error of both joint angle predictions. MCP joint error was doubly weighted to account for the smaller range of motion. Five of the 10 trials collected (one of each movement type arbitrarily selected) were used for optimization and the remaining trials were withheld for evaluation. Optimization was performed in MATLAB 2020a (MathWorks, Inc., Natick, MA) using the simulated annealing algorithm (Higginson et al., 2005) with MATLAB's *fmincon* function called every 1,000 iterations with randomly generated initial conditions, constrained by approximate physiologic ranges.

2.4. Model performance evaluation

Joint angle prediction accuracies for each model were calculated using the movement data sets withheld from the optimization. For each evaluation movement trial, Pearson's correlation coefficient (r) and root mean square error (RMSE) between measured and predicted joint angles were calculated over a continuous 16-second window from the middle of each trial.

2.5. Monte-Carlo simulations

For each subject's model, 22 simulations were performed with each parameter perturbed by randomly selecting a value from a uniform distribution scaled to the parameter's approximate physiologic range (Franko et al., 2011; Holzbaur et al., 2007; Lieber et al., 1990; Murray et al., 2000) 20,000 times, similar to previous work (Ackland et al., 2012; Bujalski et al., 2018). The number of simulations was also confirmed via pilot testing, starting with simulation sizes of 10,000 and incrementing by 1000 runs up to 25,000 runs and identifying when simulation performance converged. All other parameters were set to the

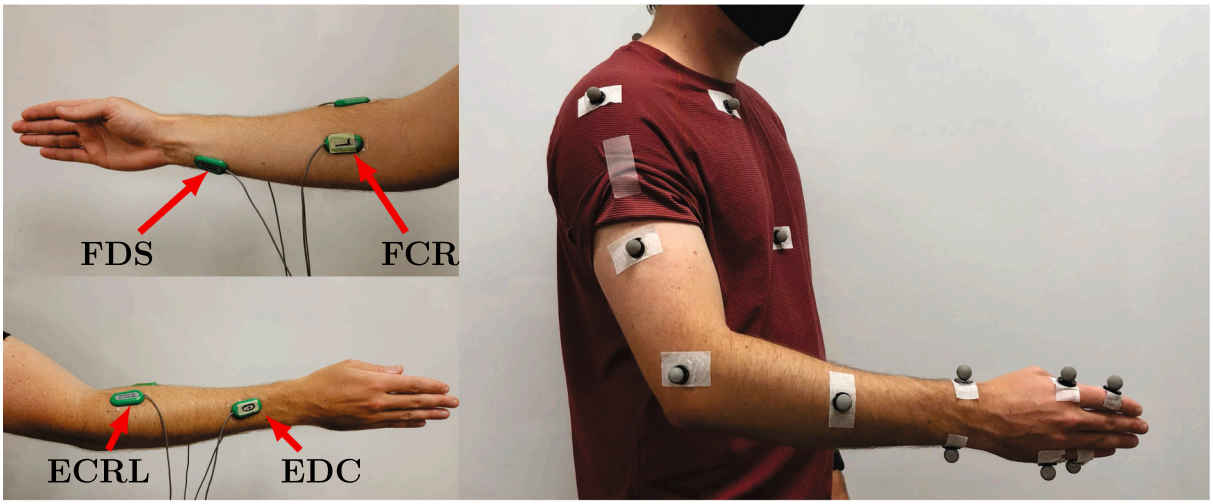

Fig. 1. Experimental setup with electrode placement shown for the *flexor carpi radialis* (FCR), *flexor digitorum superficialis* (FDS), *extensor carpi radialis longus* (ECRL), and *extensor digitorum communis* (EDC) on the left. Placement of 14 motion capture markers for tracking wrist and MCP flexion/extension is shown on the right.

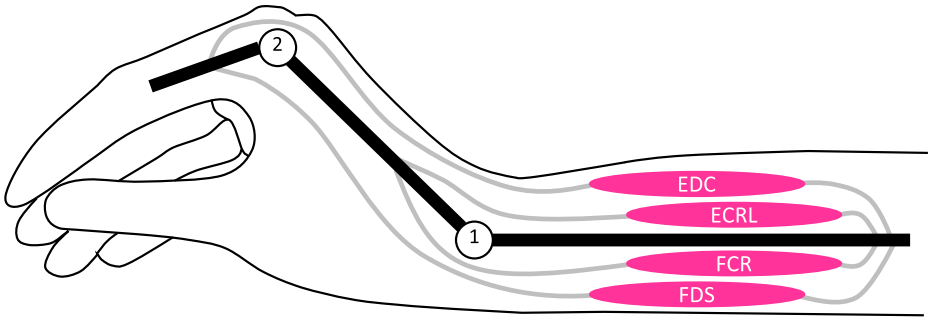

Fig. 2. A cartoon of the lumped-parameter model used in the study (Crouch and Huang, 2016). The model includes wrist flexion/extension (1) and MCP flexion/extension (2). The wrist extensors, wrist flexors, MCP extensors, and MCP flexors are lumped into ECRL, FCR, EDC, and FDS, respectively. Each muscle is modeled as a single compartment with moment arms acting at wrist and MCP joints. Moment arms at the MCP joint were fixed at 0 for ECRL and FDS since they do not cross the MCP joint.

optimized value for that subject. Additionally, all parameters of an individual muscle were simultaneously perturbed, resulting in 4 additional simulations.

2.6. Model refinement

For each muscle, the parameters were ranked from 1 (most influential) to 6 (least influential) and the sensitivity ranks were averaged across all 4 muscles to determine final rankings of parameter sensitivities across all muscles in the model. The least influential parameter was fixed to the median value of its approximate physiologic range for each muscle and the remaining parameters were optimized as previously described. This process was repeated, fixing an additional parameter in order of increasing influence until all parameters were fixed to their median value. The correlation and normalized RMSE (NRMSE; root mean square error normalized by joint range of motion) were evaluated for each model refinement. Model refinement is summarized in Fig. 3.

2.7. Sensitivity analysis informed optimization

Based on the results of the sensitivity analysis, a new optimization strategy was devised to improve model optimization by initially solving two smaller optimization problems: one for each joint. Simulated annealing was run with the same settings as described above, optimizing only the extrinsic finger muscle (EDC and FDS) parameters. The new extrinsic finger muscle parameters were then held constant, while the wrist muscle (ECRL and FCR) parameters were optimized. Finally, all parameters were allowed to be optimized simultaneously. This new

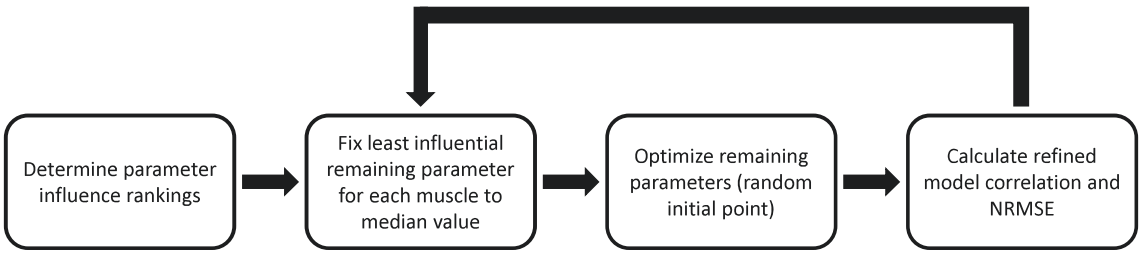

Fig. 3. A flowchart describing the model refinement process. The final parameter influence ranking from most to least influential was F_{max}, $l_{\theta=0}$, ma_{wrist}, ma_{mcp}, l_{opt}, and K. First, K was fixed to the median value for each muscle. The remaining parameters of the 4 muscles were randomly initialized and optimized. The correlation and NRMSE of the resulting refined model's predictions at each joint were calculated. Next, this process was repeated with l_{opt} fixed to a median value for each muscle (and K also fixed still). This process was repeated until all parameters were fixed to median values. The accuracies (correlation and NRMSE) of the full model and each refined model were compared.

strategy ("dual optimization strategy") was performed and the results were compared to a single optimization of all parameters ("single optimization strategy") for all subjects. This optimization strategy was compared to the baseline optimization mentioned above. The minimum costs found during optimization of each subject's model with both optimization strategies were compared, as well as the percent of 10 repeated optimizations that the optimal solution was identified by each strategy. All optimizations were performed on a desktop computer with an Intel i7 4790 K processor and 16 GB of RAM.

2.8. Data analysis

Correlation and RMSE standard deviations were calculated for each simulation where individual parameters were perturbed and were averaged across all subjects. These average standard deviations were used to rank the Hill-type parameter influences for each muscle, with higher standard deviations indicating higher sensitivity.

A paired Student's *t*-test was performed to compare the two optimization strategies' performance, as well as compare the performance of the models generated with different numbers of parameters held constant to the full model.

3. Results

3.1. Sensitivity analysis

As correlation results showed the same trends, only RMSE results are presented for brevity. Sensitivities for model parameters were similar for the wrist muscles. For ECRL and FCR, wrist angle accuracy had higher sensitivity to F_{max} (12.38°±6.71° and 18.25°±5.56°, respectively), $l_{\theta=0}$ (5.99°±4.61° and 9.55°±2.93°, respectively), and ma_{wrist} (14.38°±8.48° and 7.00°±3.82°, respectively), and lower sensitivity to l_{opt} (1.21°±1.27° and 1.36°±1.17°, respectively) and K (0.85°±1.34° and 1.23°±0.76°, respectively; Fig. 4 and Table 1). Wrist angle accuracy was insensitive to all parameters of the extrinsic finger muscles (EDC and FDS). Simultaneous perturbation of all parameters for a single muscle resulted in slightly higher RMSE variance at the wrist joint than the most sensitive parameter for each muscle.

Sensitivities of MCP joint angle accuracy are summarized in Table 2 and Fig. 4. MCP angle accuracy sensitivities varied by muscle and were similar to those observed for the wrist angle accuracy. For EDC and FDS, MCP kinematic prediction accuracy had higher sensitivity to F_{max} (11.09°±5.98° and 11.60°±5.06°, respectively), $l_{\theta=0}$ (3.23°±2.24° and 11.82°±6.05°, respectively), and ma_{mcp} (6.17°±5.22° and 12.39°±8.10°, respectively), and lower sensitivity to l_{opt} (0.47°±0.50° and 2.57°±2.23°, respectively) and K (0.37°±0.53° and 0.49°±0.87°, respectively). Kinematic prediction accuracy at the MCP joint was also sensitive to the parameters of ECRL and FCR (F_{max}, $l_{\theta=0}$, and ma_{wrist}; Table 2). Simultaneous perturbation of all parameters for a single muscle resulted in slightly higher variation in prediction RMSE at the MCP joint than the most sensitive parameter for each muscle.

The sensitivity ranks of each parameter were averaged across all muscles and both joints to determine the final sensitivity ranks. The final parameter rankings averaged across all muscles from most to least sensitive are F_{max}, $l_{\theta=0}$, ma_{wrist}, ma_{mcp}, l_{opt}, and K.

3.2. Model refinement

Fig. 5 shows model performance across all subjects when different number of parameters are removed from the optimization problem. Optimization of the full 22 parameter model resulted in prediction correlations of 0.90 ± 0.05 and 0.74 ± 0.20 for the wrist and MCP joints,

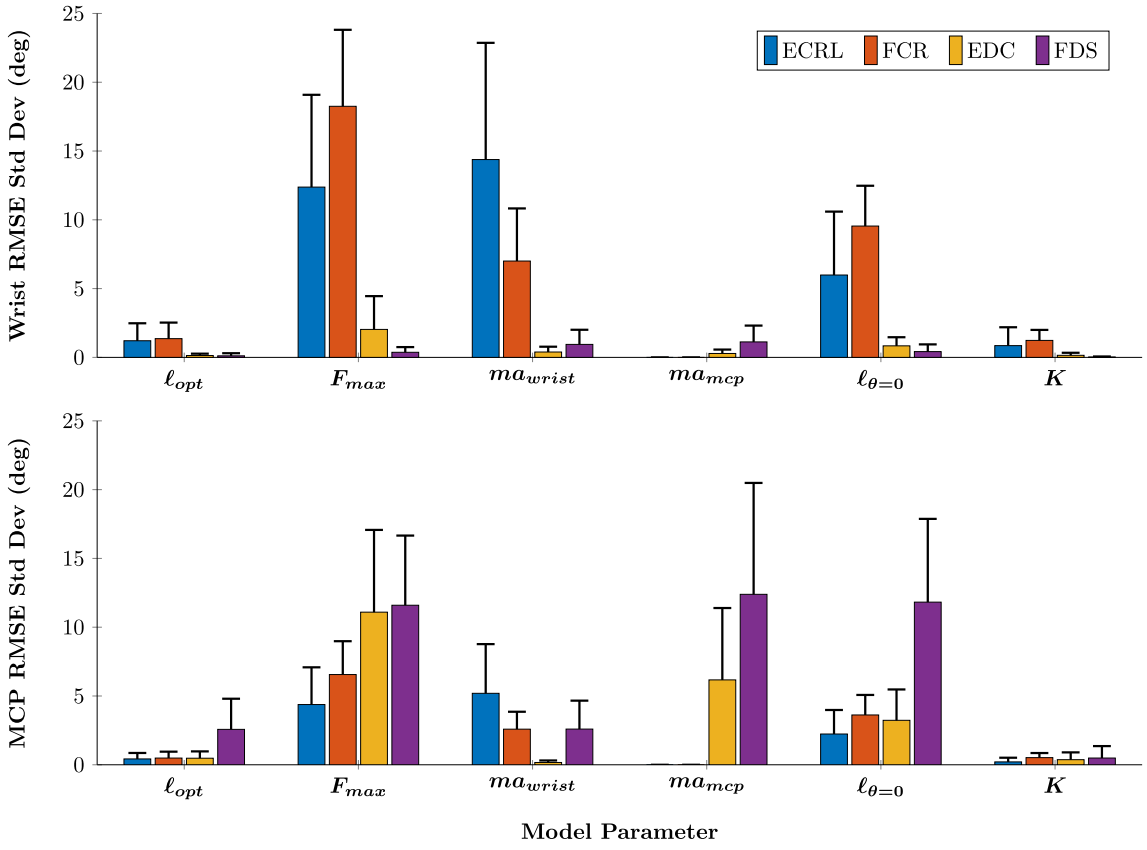

Fig. 4. Standard deviation of model prediction RMSE at the wrist (top) and MCP (bottom) joints for the Monte-Carlo simulation of each parameter for ECRL (blue), FCR (orange), EDC (yellow), and FDS (purple). Higher standard deviation indicates greater influence by that parameter. Error bars indicate simulation standard deviation.

Table 1
Mean ($\mu(\sigma)$) and maximum standard deviation (σ_{max}) of wrist joint angle prediction RMSE (in degrees) for extensor carpi radialis longus, flexor carpi radialis, extensor digitorum communis, and flexor digitorum superficialis. The parameter name shown above each column indicates a Monte-Carlo simulation for that parameter of the muscle being perturbed individually for each subject. Parameters are listed in order of increasing sensitivities from left to right, with combined perturbation of all muscle parameters in the far-right column.

Wrist RMSE	Parameter Sensitivity Rank						Combined Parameter Perturbation
	Least Sensitive → Most Sensitive						
	6	5	4	3	2	1	
	Extensor Carpi Radialis Longus						
	ma_{MCP}	K	l_{opt}	$l_{\theta=0}$	F_{max}	ma_{wrist}	
$\mu(\sigma)$	–	0.85	1.21	5.99	12.38	14.38	17.12
σ_{max}	–	6.08	4.60	24.98	25.76	33.38	37.39
	Flexor Carpi Radialis						
	ma_{MCP}	K	l_{opt}	ma_{wrist}	$l_{\theta=0}$	F_{max}	
$\mu(\sigma)$	–	1.23	1.36	7.00	9.55	18.25	20.31
σ_{max}	–	3.08	5.57	18.68	16.58	29.27	28.05
	Extensor Digitorum Communis						
	l_{opt}	K	ma_{MCP}	ma_{wrist}	$l_{\theta=0}$	F_{max}	
$\mu(\sigma)$	0.14	0.15	0.29	0.39	0.84	2.03	2.37
σ_{max}	0.58	0.86	0.96	1.48	3.07	8.98	8.08
	Flexor Digitorum Superficialis						
	K	l_{opt}	F_{max}	$l_{\theta=0}$	ma_{wrist}	ma_{MCP}	
$\mu(\sigma)$	0.02	0.11	0.37	0.42	0.94	1.12	6.55
σ_{max}	0.18	1.42	1.41	2.50	6.20	5.07	20.50

Table 2
Mean ($\mu(\sigma)$) and maximum standard deviation (σ_{max}) of MCP joint angle prediction RMSE (in degrees) for extensor carpi radialis longus, flexor carpi radialis, extensor digitorum communis, and flexor digitorum superficialis. The parameter name shown above each column indicates a Monte-Carlo simulation for that parameter of the muscle being perturbed individually for each subject. Parameters are listed in order of increasing sensitivities from left to right, with combined perturbation of all muscle parameters in the far-right column. MCP moment arm is left blank for the wrist muscles, as this parameter was fixed at zero.

MCP RMSE	Parameter Sensitivity Rank						Combined Parameter Perturbation
	Least Sensitive → Most Sensitive						
	6	5	4	3	2	1	
	Extensor Carpi Radialis Longus						
	ma_{MCP}	K	l_{opt}	$l_{\theta=0}$	F_{max}	ma_{wrist}	
$\mu(\sigma)$	–	0.21	0.42	2.24	4.38	5.19	6.57
σ_{max}	–	1.84	1.89	7.08	11.49	15.12	16.41
	Flexor Carpi Radialis						
	ma_{MCP}	l_{opt}	K	ma_{wrist}	$l_{\theta=0}$	F_{max}	
$\mu(\sigma)$	–	0.49	0.52	2.59	3.62	6.56	7.39
σ_{max}	–	2.43	1.20	5.94	6.53	12.53	12.43
	Extensor Digitorum Communis						
	ma_{wrist}	K	l_{opt}	$l_{\theta=0}$	ma_{MCP}	F_{max}	
$\mu(\sigma)$	0.17	0.37	0.48	3.23	6.17	11.09	12.27
σ_{max}	0.86	2.97	2.45	9.90	27.51	29.00	33.08
	Flexor Digitorum Superficialis						
	K	l_{opt}	ma_{wrist}	F_{max}	$l_{\theta=0}$	ma_{MCP}	
$\mu(\sigma)$	0.49	2.57	2.60	11.60	11.82	12.39	18.66
σ_{max}	4.51	7.83	8.82	22.36	26.18	34.66	31.37

respectively, and prediction normalized RMSE (NRMSE) of 0.177 ± 0.031 and 0.182 ± 0.064 for the wrist and MCP joints, respectively. Fixing K and l_{opt} to median values for all muscles and optimizing the remaining parameters resulted in similar model performance for both the wrist (correlation: $p = 0.96$; NRMSE: $p = 0.16$) and MCP (correlation: $p = 0.51$; NRMSE: $p = 0.60$) compared to the model with all parameters optimized. A significant increase in NRMSE was observed for the MCP joint when ma_{mcp} was fixed to its median value in addition to K and l_{opt} ($p = 0.02$; Fig. 5, dashed orange line). Additionally fixing ma_{wrist} to its median value results in a significant increase in NRMSE for the wrist joint ($p < 0.001$), as indicated by the dashed blue line in Fig. 5, and a significant decrease in correlation for both the wrist ($p = 0.03$) and MCP ($p = 0.007$) when compared to the model with all parameters optimized.

Fig. 6 shows representative examples of predictions for both joints for the original model optimization (6 parameters per muscle) and two simplified model optimizations (4 parameters per muscle and 2 parameters per muscle). While wrist angle predictions are qualitatively similar for all models shown in Fig. 6 (r = 0.98, 0.98, and 0.95 for 6, 4, and 2 parameters per muscle, respectively), the degradation of MCP angle accuracy with fewer optimized parameters is apparent (r = 0.92,

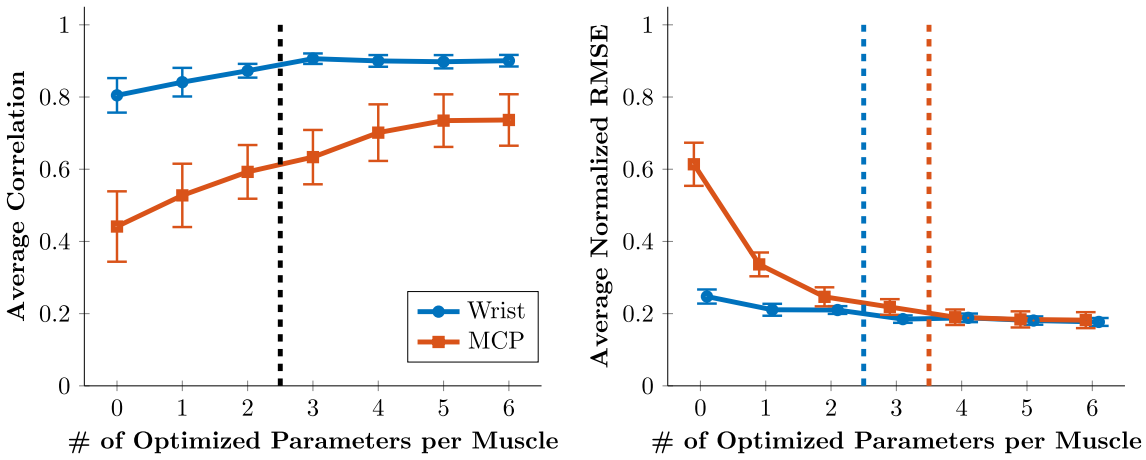

Fig. 5. Model predictive correlation (left) and normalized RMSE (right) for the wrist (blue) and MCP (orange) joints for different numbers of optimizable parameters per muscle. On the x-axis 0 indicates all parameters were assigned a median value, 1 indicates the most influential parameter (F_{max}) was optimized for each muscle, up to 6 indicating inclusion of the least influential parameter (K) in the optimization. Order of parameter inclusion in order from most to least sensitive is F_{max}, $l_{\theta=0}$, ma_{wrist}, ma_{mcp}, l_{opt}, and K. No significant decrease in correlation compared to the full model is observed until only the 2 most influential parameters are optimized per muscle (black dashed line) for the wrist ($r = 0.87 \pm 0.05$, $p = 0.03$) and MCP ($r = 0.59 \pm 0.21$, $p = 0.007$). A significant increase in normalized RMSE is seen with only the 3 most influential parameters optimized per muscle for the MCP joint (orange dashed line; NRMSE $= 0.218 \pm 0.062$, $p = 0.02$) and 2 parameters optimized per muscle (blue dashed line; NRMSE $= 0.210 \pm 0.031$, $p < 0.001$) for the wrist joint. Error bars indicate 95% confidence intervals.

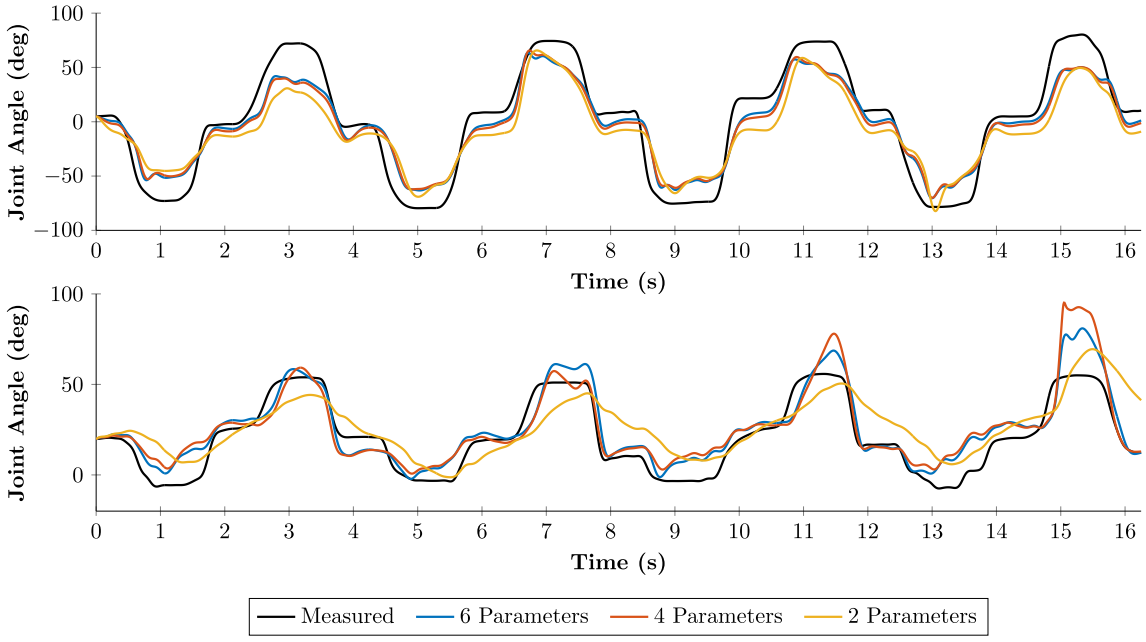

Fig. 6. Representative comparison of estimated kinematics from a 6 parameters per muscle model (blue), 4 parameters per muscle model (orange), and 2 parameters per muscle model (yellow) to measured kinematics (black) of the wrist (top) and MCP (bottom) joints from subject AB01. Qualitatively, the 6 and 4 parameters per muscle models' predictions were similar, while the 2 parameter per muscle model performance was noticeably worse, highlighting the difference in performance between the models of different complexities.

0.87, and 0.79 for 6, 4, and 2 parameters per muscle, respectively).

3.3. Sensitivity analysis informed optimization

Based on the relatively small influence that MCP muscle parameters exert on the wrist joint predictions, we developed and tested the dual optimization strategy described above. The dual optimization strategy achieved either the same or better optimal solution for all subjects, as evidenced by the lower cost function values (Fig. 7, top). Additionally, the dual optimization strategy was able to successfully identify the optimal solutions at a significantly higher rate of $27.3 \pm 19.5\%$ than the single optimization strategy rate of $6.4 \pm 8.1\%$ ($p = 0.004$), although the dual optimization strategy did require more computational time than the single optimization strategy (Dual: 431 ± 121 s; Single: 209 ± 25 s; $p < 0.001$).

4. Discussion

Previous sensitivity analyses on musculoskeletal models have focused on determining model parameter effects on force generation and global kinematic measures, such as center of mass acceleration in gait models (Ackland et al., 2012). In contrast, this study evaluated sensitivity to musculoskeletal model parameters for prediction of upper extremity joint kinematics. Study of upper extremity models is needed as

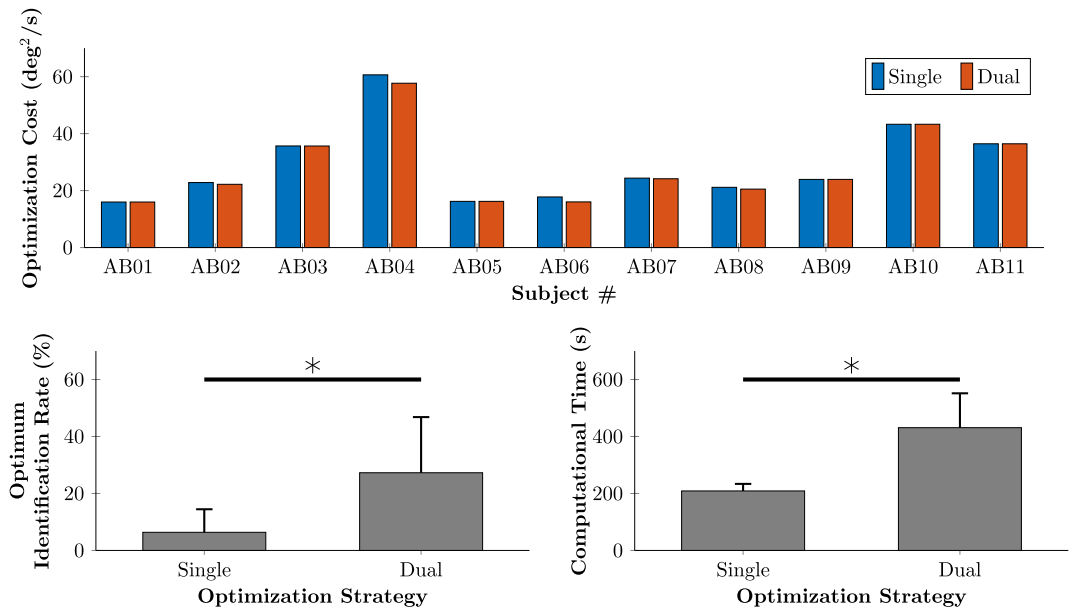

Fig. 7. The minimum optimization cost function value (top) for the single (blue) and dual (orange) optimization strategies show the dual strategy identifies either the same solution, or a better solution for all subjects. The identification rate of the optimal solution (left) and computational time (right) of both strategies are compared. Identification rate was determined by applying each optimization strategy 10 times and calculating the percentage of those 10 optimizations the optimal solution was identified. The dual optimization strategy identifies the optimal solution at a significantly higher rate (single: 6.4 ± 8.1%; dual: 27.3 ± 19.5%; $p = 0.004$). Computational time is increased by the dual optimization strategy (dual: 431 ± 121 s; single: 209 ± 25 s; $p < 0.001$) but is still at a reasonable value at <10 min for a single subject.

many are purely open kinetic chain, as no external force is modeled, while the lower extremity gait models frequently studied are closed kinetic chains, potentially altering parameter sensitivities between lower and upper extremity models. Joint angle prediction accuracy sensitivities were interrogated instead of force generation capacities because the desired function of the model studied is to accurately predict joint kinematics, which has been used for rehabilitation related applications, such as assistive device control (Blana et al., 2017; Crouch and Huang, 2016; Lambrecht et al., 2009). Directly analyzing the desired final output of the model (kinematics) instead of an intermediate value (force) accounts for the effects of forward dynamic and computational error effects on the influence of each parameter. Therefore, our approach can directly benefit the applications of musculoskeletal model for accurate motion prediction and can inform the efficient design and personalization of musculoskeletal model-based EMG decoding system for various HMI applications.

While sensitivity to parameters varied by muscle, some clear trends emerged. Wrist joint kinematic prediction accuracy was found to be highly sensitive to F_{max}, $l_{\theta=0}$, and ma_{wrist} for the two wrist muscles (Fig. 4 and Table 1). A muscle's force–length curve magnitude is scaled by F_{max} and greatly affects the force generation of a muscle and its resulting kinematics. The parameter $l_{\theta=0}$ is analogous to tendon slack length, which has consistently been identified as highly influential for muscle force generation (Ackland et al., 2012; Bujalski et al., 2018). Tendon slack length sets the operating region of a muscle's force–length curve (Zajac, 1989), thus substantially altering the force-generating potential of a muscle and greatly changing the kinematics predicted at the wrist joint. Moment arm determines the size of the operating region of a muscle's force–length curve, and therefore similarly influences its force-generating capacity (Murray et al., 2000). It is worth noting some of the magnitudes of the RMSE observed in Fig. 4 and Tables 1 and 2 are large in the context of the wrist and MCP joints. However, the correlation of the predictions remains strong (Fig. 5), thus allowing for feasible real-time control as previously demonstrated (Crouch et al., 2018; Crouch and Huang, 2017).

In contrast, previous analyses of lower extremity model kinematics found moment arms to have significantly less influence on muscle force production. The significant influence of moment arm on wrist kinematics, compared to the lower extremity, may potentially arise because the upper extremity segments have much smaller masses and moments of inertia compared to the lower extremity, making the kinematics more sensitive to changes in torque. Adjusting moment arms will lead to changes in joint torques, thus causing greater changes in kinematics due to the smaller inertias.

By systematically studying the sensitivity of joint angle prediction accuracy for both joints and removing the least sensitive parameters from the optimization scheme, we were able to simplify the model studied. Removal of the two least influential parameters (K and l_{opt}) for each muscle greatly reduced the complexity of the model (and optimization) from 22 parameters to 14 parameters without sacrificing model performance. As seen in Fig. 5, predictive correlation for both joints did not significantly decline until the 4 least sensitive parameters were held constant. However, NRMSE behaved differently between joints, with 3 constant parameters causing a significant increase in predicted MCP angle error. These results demonstrate a systematic approach to guide model refinement for clinical applications to avoid unnecessary complexity in the system without sacrificing performance. This systematic approach works toward eliminating the barrier that optimization of models (even simplified ones like the one evaluated here) presents to clinical implementation, such as the control of upper extremity rehabilitation devices.

While it is known extrinsic finger muscles contribute to wrist moments (Lieber et al., 1996), the two extrinsic finger muscles modeled here did not strongly influence wrist angle accuracy when perturbations were applied to all parameters of these muscles (Fig. 4 and Table 1), despite crossing the wrist joint and being active during isolated wrist motion trials. This is possibly due to the higher moment of inertia of the palm segment compared to the finger segment resulting in less kinematic perturbation (Crouch and Huang, 2016). Nevertheless, MCP joint angle predictions were highly sensitive to parameters of the wrist muscles, despite no direct action at the MCP joint (Fig. 4 and Table 2). This may be a result of the two-link nature of the model. The states of EDC and FDS

(fiber length and velocity) depend on the kinematics of the wrist joint. Therefore, while ECRL and FCR do not act directly on the MCP joint, the strong influence their parameters exert on MCP joint kinematics is likely due to their strong influence on wrist joint kinematics. These observed sensitivities across joints motivated the formulation of the dual optimization strategy: we initially optimize the extrinsic finger and wrist muscle parameters separately, as lower dimensional optimization problems are often faster and easier to solve. The dual optimization strategy showed itself to be more robust than a single optimization of all parameters simultaneously, as it was able to more reliably identify the optimal solution (Fig. 7). While computational time increased, optimization required <10 min total on average. The benefits of the dual optimization strategy highlight how the 2-DOF nature of the model and observing the sensitivities of each degree of freedom were able to inform model improvement and simplify computations.

This study is not without its limitations. The sensitivity analysis was limited to Hill-type and musculoskeletal geometry parameters. The model studied is also influenced by the modeled inertial properties of the hand/wrist and excitation-activation dynamics. Analyses of the influence of these parameters' effects on kinematic prediction accuracy are warranted and will be the subject of future works. The study was also limited by the design of the model itself. The muscles modeled did not include an elastic tendon, instead treating the tendon as rigid. Additionally, the moment arms of each muscle were held constant with respect to joint angle. While some muscles in the model have relatively constant moment arm (FCR and EDC), others (ECRL and FDS) do not (An et al., 1983; Gonzalez et al., 1997). This simplification could potentially explain the observed sensitivity to moment arms, as the moment arm potentially is less accurate in certain joint angles, while in a more accurate representation, moment arm depends on the muscle path and varies with joint angle. Finally, the inertial properties of the palm and finger segments are approximated as two cylinders. These simplifications can be improved upon in future works but may require additional computational resources, making the model more difficult to implement in real-time as an HMI.

5. Conclusions

Sensitivity analyses provide important insight into which parameters exert the most influence on a model's performance. In this study, we examined the sensitivity of an EMG-driven lumped-parameter upper extremity model to Hill-type and musculoskeletal geometry parameters. While sensitivity was muscle dependent, we identified maximum isometric force and tendon slack length as highly influential parameters, consistent with previous force-based analyses. Additionally, muscle moment arm exerted significant influence on kinematic prediction accuracy, while previous work found moment arm exerted little relative influence for force generation. This demonstrated the importance of evaluating model performance according to the desired application and will provide a framework for future analyses as models become more widely used for kinematic predictions and HMIs. While other work has studied the optimization of upper extremity model parameters (Goislard de Monsabert et al., 2020; Goislard De Monsabert et al., 2018), these too have focused on optimizing force generation, and to the best of our knowledge, this is the first such analysis that examined an upper extremity model's sensitivity in terms of local joint kinematic prediction accuracy.

In addition to the biomechanical implications discussed, this study demonstrated and quantified the interaction of multiple degrees of freedoms in a model by observing performance of each joint's prediction accuracy in conditions of both isolated and simultaneous motion, allowing us to greatly reduce model complexity. Furthermore, the sensitivity analysis revealed the wrist joint prediction accuracy was not strongly influenced by the parameters of the 2 included extrinsic finger muscles, as modeled in this study. These results inspired a custom optimization approach for the model studied, demonstrating how such an analysis can be applied to better inform optimization of models across rehabilitation fields.

CRediT authorship contribution statement

Robert Hinson: Writing – review & editing, Writing – original draft, Visualization, Validation, Software, Methodology, Investigation, Formal analysis, Data curation, Conceptualization. **Katherine Saul:** Writing – review & editing, Visualization, Validation, Supervision, Methodology, Formal analysis, Conceptualization. **Derek Kamper:** Writing – review & editing, Visualization, Validation, Methodology, Formal analysis, Conceptualization. **He Huang:** Writing – review & editing, Visualization, Validation, Supervision, Project administration, Methodology, Funding acquisition, Formal analysis, Conceptualization.

Declaration of Competing Interest

The authors declare that they have no known competing financial interests or personal relationships that could have appeared to influence the work reported in this paper.

Acknowledgements

This work was supported by the following National Science Founds (NSF) grants: NSF #1856441, NSF #1527202, and NSF #1637892. It was also supported by the Department of Defense (DOD) #W81XWH15C0125.

References

Ackland, D.C., Lin, Y.-C., Pandy, M.G., 2012. Sensitivity of model predictions of muscle function to changes in moment arms and muscle–tendon properties: A Monte-Carlo analysis. J. Biomech. 45, 1463–1471. https://doi.org/10.1016/j.jbiomech.2012.02.023.

An, K.N., Ueba, Y., Chao, E.Y., Cooney, W.P., Linscheid, R.L., 1983. Tendon excursion and moment arm of index finger muscles. J. Biomech. 16, 419–425. https://doi.org/10.1016/0021-9290(83)90074-X.

Blana, D., Chadwick, E.K., van den Bogert, A.J., Murray, W.M., 2017. Real-time simulation of hand motion for prosthesis control. Comput. Methods Biomech. Biomed. Eng. 20, 540–549. https://doi.org/10.1080/10255842.2016.1255943.

Blana, D., van den Bogert, A.J., Murray, W.M., Ganguly, A., Krasoulis, A., Nazarpour, K., Chadwick, E.K., 2020. Model-Based Control of Individual Finger Movements for Prosthetic Hand Function. IEEE Trans. Neural Syst. Rehabil. Eng. 28, 612–620. https://doi.org/10.1109/TNSRE.2020.2967901.

Boey, H., van Rossom, S., Verfaillie, S., Sloten, J. vander, Jonkers, I., 2022. Maximal lateral ligament strain and loading during functional activities: Model-based insights for ankle sprain prevention and rehabilitation. Clinical Biomechanics 94, 105623. https://doi.org/10.1016/J.CLINBIOMECH.2022.105623.

Bueno, D.R., Montano, L., 2017. Neuromusculoskeletal model self-calibration for on-line sequential Bayesian moment estimation. J. Neural Eng. 14 https://doi.org/10.1088/1741-2552/aa58f5.

Bujalski, P., Martins, J., Stirling, L., 2018. A Monte Carlo analysis of muscle force estimation sensitivity to muscle-tendon properties using a Hill-based muscle model. J. Biomech. 79, 67–77. https://doi.org/10.1016/j.jbiomech.2018.07.045.

Crouch, D.L., Huang, H., 2016. Lumped-parameter electromyogram-driven musculoskeletal hand model: A potential platform for real-time prosthesis control. J. Biomech. 49, 3901–3907. https://doi.org/10.1016/j.jbiomech.2016.10.035.

Crouch, D.L., Huang, H. (Helen), 2017. Musculoskeletal model-based control interface mimics physiologic hand dynamics during path tracing task. Journal of Neural Engineering 14, 036008. https://doi.org/10.1088/1741-2552/aa61bc.

Crouch, D.L., Pan, L., Filer, W., Stallings, J.W., Huang, H., 2018. Comparing Surface and Intramuscular Electromyography for Simultaneous and Proportional Control Based on a Musculoskeletal Model: A Pilot Study. IEEE Trans. Neural Syst. Rehabil. Eng. 26, 1735–1744. https://doi.org/10.1109/TNSRE.2018.2859833.

Davico, G., Pizzolato, C., Lloyd, D.G., Obst, S.J., Walsh, H.P.J., Carty, C.P., 2020. Increasing level of neuromusculoskeletal model personalisation to investigate joint contact forces in cerebral palsy: A twin case study. Clin. Biomech. 72, 141–149. https://doi.org/10.1016/j.clinbiomech.2019.12.011.

de Groote, F., van Campen, A., Jonkers, I., de Schutter, J., 2010. Sensitivity of dynamic simulations of gait and dynamometer experiments to hill muscle model parameters of knee flexors and extensors. J. Biomech. 43, 1876–1883. https://doi.org/10.1016/j.jbiomech.2010.03.022.

Delp, S.L., Anderson, F.C., Arnold, A.S., Loan, P., Habib, A., John, C.T., Guendelman, E., Thelen, D.G., 2007. OpenSim: Open-source software to create and analyze dynamic simulations of movement. IEEE Trans. Biomed. Eng. 54, 1940–1950. https://doi.org/10.1109/TBME.2007.901024.

Delp, S.L., Loan, J.P., Hoy, M.G., Zajac, F.E., Topp, E.L., Rosen, J.M., 1990. An interactive graphics-based model of the lower extremity to study orthopaedic surgical procedures. IEEE Trans. Biomed. Eng. 37, 757–767. https://doi.org/10.1109/10.102791.

Durandau, G., Farina, D., Asín-Prieto, G., Dimbwadyo-Terrer, I., Lerma-Lara, S., Pons, J. L., Moreno, J.C., Sartori, M., 2019. Voluntary control of wearable robotic exoskeletons by patients with paresis via neuromechanical modeling. J. NeuroEng. Rehabil. 16, 1–18. https://doi.org/10.1186/s12984-019-0559-z.

Eilenberg, M.F., Geyer, H., Herr, H., 2010. Control of a powered ankle-foot prosthesis based on a neuromuscular model. IEEE Trans. Neural Syst. Rehabil. Eng. 18, 164–173. https://doi.org/10.1109/TNSRE.2009.2039620.

Franko, O.I., Winters, T.M., Tirrell, T.F., Hentzen, E.R., Lieber, R.L., 2011. Moment arms of the human digital flexors. J. Biomech. 44, 1987–1990. https://doi.org/10.1016/j.jbiomech.2011.04.025.

Fregly, B.J., 2021. A Conceptual Blueprint for Making Neuromusculoskeletal Models Clinically Useful. Applied Sciences 11, 2037. https://doi.org/10.3390/app11052037.

Fregly, B.J., Reinbolt, J.A., Rooney, K.L., Mitchell, K.H., Chmielewski, T.L., 2007. Design of patient-specific gait modifications for knee osteoarthritis rhabilitation. IEEE Trans. Biomed. Eng. 54, 1687–1695. https://doi.org/10.1109/TBME.2007.891934.

Goislard De Monsabert, B., Edwards, D., Shah, D., Kedgley, A., 2018. Importance of Consistent Datasets in Musculoskeletal Modelling: A Study of the Hand and Wrist. Ann. Biomed. Eng. 46, 71–85. https://doi.org/10.1007/s10439-017-1936-z.

Goislard de Monsabert, B., Hauraix, H., Caumes, M., Herbaut, A., Berton, E., Vigouroux, L., 2020. Modelling force-length-activation relationships of wrist and finger extensor muscles. Med. Biol. Eng. Compu. 58, 2531–2549. https://doi.org/10.1007/S11517-020-02239-0/FIGURES/8.

Gonzalez, R. v., Buchanan, T.S., Delp, S.L., 1997. How muscle architecture and moment arms affect wrist flexion-extension moments. Journal of Biomechanics 30, 705–712. https://doi.org/10.1016/S0021-9290(97)00015-8.

Higginson, J.S., Neptune, R.R., Anderson, F.C., 2005. Simulated parallel annealing within a neighborhood for optimization of biomechanical systems. J. Biomech. 38, 1938–1942. https://doi.org/10.1016/J.JBIOMECH.2004.08.010.

Hoang, H.X., Diamond, L.E., Lloyd, D.G., Pizzolato, C., 2019. A calibrated EMG-informed neuromusculoskeletal model can appropriately account for muscle co-contraction in the estimation of hip joint contact forces in people with hip osteoarthritis. J. Biomech. 83, 134–142. https://doi.org/10.1016/j.jbiomech.2018.11.042.

Holzbaur, K.R.S., Murray, W.M., Delp, S.L., 2005. A model of the upper extremity for simulating musculoskeletal surgery and analyzing neuromuscular control. Ann. Biomed. Eng. 33, 829–840. https://doi.org/10.1007/s10439-005-3320-7.

Holzbaur, K.R.S., Murray, W.M., Gold, G.E., Delp, S.L., 2007. Upper limb muscle volumes in adult subjects. J. Biomech. 40, 742–749. https://doi.org/10.1016/j.jbiomech.2006.11.011.

Kotsifaki, A., van Rossom, S., Whiteley, R., Korakakis, V., Bahr, R., D'Hooghe, P., Papakostas, E., Sideris, V., Farooq, A., Jonkers, I., 2022. Between-Limb Symmetry in ACL and Tibiofemoral Contact Forces in Athletes After ACL Reconstruction and Clearance for Return to Sport. Orthopaedic Journal of Sports Medicine 10, 232596712210847. https://doi.org/10.1177/23259671221084742.

Lambrecht, J.M., Audu, M.L., Triolo, R.J., Kirsch, R.F., 2009. Musculoskeletal model of trunk and hips for development of seated-posture-control neuroprosthesis. The Journal of Rehabilitation Research and Development 46, 515. https://doi.org/10.1682/JRRD.2007.08.0115.

Lieber, R.L., Amiel, D., Kaufman, K.R., Whitney, J., Gelberman, R.H., 1996. Relationship between joint motion and flexor tendon force in the canine forelimb. The Journal of Hand Surgery 21, 957–962. https://doi.org/10.1016/S0363-5023(96)80299-1.

Lieber, R.L., Fazeli, B.M., Botte, M.J., 1990. Architecture of selected wrist flexor and extensor muscles. J Hand Surg Am 15, 244–250. https://doi.org/10.1016/0363-5023(90)90103-x.

Lloyd, D.G., Besier, T.F., 2003. An EMG-driven musculoskeletal model to estimate muscle forces and knee joint moments in vivo. J. Biomech. 36, 765–776. https://doi.org/10.1016/S0021-9290(03)00010-1.

Manal, K., Gonzalez, R. v., Lloyd, D.G., Buchanan, T.S., 2002. A real-time EMG-driven virtual arm. Computers in Biology and Medicine 32, 25–36. https://doi.org/10.1016/S0010-4825(01)00024-5.

Modenese, L., Ceseracciu, E., Reggiani, M., Lloyd, D.G., 2016. Estimation of musculotendon parameters for scaled and subject specific musculoskeletal models using an optimization technique. J. Biomech. 49, 141–148. https://doi.org/10.1016/j.jbiomech.2015.11.006.

Murray, W.M., Buchanan, T.S., Delp, S.L., 2000. The isometric functional capacity of muscles that cross the elbow. J. Biomech. 33, 943–952. https://doi.org/10.1016/S0021-9290(00)00051-8.

Pan, L., Crouch, D.L., Huang, H., 2018. Myoelectric Control Based on a Generic Musculoskeletal Model: Toward a Multi-User Neural-Machine Interface. IEEE Trans. Neural Syst. Rehabil. Eng. 26, 1435–1442. https://doi.org/10.1109/TNSRE.2018.2838448.

Pizzolato, C., Lloyd, D.G., Sartori, M., Ceseracciu, E., Besier, T.F., Fregly, B.J., Reggiani, M., 2015. CEINMS: A toolbox to investigate the influence of different neural control solutions on the prediction of muscle excitation and joint moments during dynamic motor tasks. J. Biomech. 48, 3929–3936. https://doi.org/10.1016/j.jbiomech.2015.09.021.

Rajagopal, A., Kidziński, Ł., McGlaughlin, A.S., Hicks, J.L., Delp, S.L., Schwartz, M.H., 2020. Pre-operative gastrocnemius lengths in gait predict outcomes following gastrocnemius lengthening surgery in children with cerebral palsy. PLoS ONE 15, e0233706. https://doi.org/10.1371/journal.pone.0233706.

Redl, C., Gfoehler, M., Pandy, M.G., 2007. Sensitivity of muscle force estimates to variations in muscle-tendon properties. Hum. Mov. Sci. 26, 306–319. https://doi.org/10.1016/j.humov.2007.01.008.

Sartori, M., Durandau, G., Došen, S., Farina, D., 2018. Robust simultaneous myoelectric control of multiple degrees of freedom in wrist-hand prostheses by real-time neuromusculoskeletal modeling. J. Neural Eng. 15, 066026 https://doi.org/10.1088/1741-2552/aae26b.

Saxby, D.J., Killen, B.A., Pizzolato, C., Carty, C.P., Diamond, L.E., Modenese, L., Fernandez, J., Davico, G., Barzan, M., Lenton, G., da Luz, S.B., Suwarganda, E., Devaprakash, D., Korhonen, R.K., Alderson, J.A., Besier, T.F., Barrett, R.S., Lloyd, D. G., 2020. Machine learning methods to support personalized neuromusculoskeletal modelling. Biomech. Model. Mechanobiol. 19, 1169–1185. https://doi.org/10.1007/s10237-020-01367-8.

Scovil, C.Y., Ronsky, J.L., 2006. Sensitivity of a Hill-based muscle model to perturbations in model parameters. J. Biomech. 39, 2055–2063. https://doi.org/10.1016/j.jbiomech.2005.06.005.

Valente, G., Taddei, F., Jonkers, I., 2013. Influence of weak hip abductor muscles on joint contact forces during normal walking: Probabilistic modeling analysis. J. Biomech. 46, 2186–2193. https://doi.org/10.1016/J.JBIOMECH.2013.06.030.

Zajac, F.E., 1989. Muscle and tendon: properties, models, scaling, and application to biomechanics and motor control. Crit. Rev. Biomed. Eng. 17, 359–411.

Zuk, M., Syczewska, M., Pezowicz, C., 2018. Influence of uncertainty in selected musculoskeletal model parameters on muscle forces estimated in inverse dynamics-based static optimization and hybrid approach. J. Biomech. Eng. 140, 1–12. https://doi.org/10.1115/1.4040943.